CLIMATOLOGY

Evidence for extreme export of Arctic sea ice leading the abrupt onset of the Little Ice Age

Martin W. Miles[1,2]*, Camilla S. Andresen[3†], Christian V. Dylmer[4†]

Arctic sea ice affects climate on seasonal to decadal time scales, and models suggest that sea ice is essential for longer anomalies such as the Little Ice Age. However, empirical evidence is fragmentary. Here, we reconstruct sea ice exported from the Arctic Ocean over the past 1400 years, using a spatial network of proxy records. We find robust evidence for extreme export of sea ice commencing abruptly around 1300 CE and terminating in the late 1300s. The exceptional magnitude and duration of this "Great Sea-Ice Anomaly" was previously unknown. The pulse of ice along East Greenland resulted in downstream increases in polar waters and ocean stratification, culminating ~1400 CE and sustained during subsequent centuries. While consistent with external forcing theories, the onset and development are notably similar to modeled spontaneous abrupt cooling enhanced by sea-ice feedbacks. These results provide evidence that marked climate changes may not require an external trigger.

INTRODUCTION

The reduction in the Arctic sea-ice cover observed in recent decades is considered a leading indicator of climate change (*1*). Sea ice is, however, not only merely a passive responder but also an active agent of climate-system changes on seasonal to decadal time scales. Recently, seasonal-scale changes in atmospheric circulation patterns have been linked to reduced Arctic sea ice, leading to cold winters (*2*, *3*). On a decadal scale, the Great Salinity Anomaly (GSA) of the 1960s to 1970s (*4*) was the result of enhanced export of sea ice and freshwater from the Arctic Ocean through Fram Strait between Greenland and Svalbard, then carried to the subpolar North Atlantic by the East Greenland Current (EGC). There are also indications of a larger GSA during the late 19th to early 20th century (*5*, *6*), suggesting that these are recurring events.

Numerical model experiments have suggested that feedbacks associated with increased sea-ice cover in the region—possibly in response to volcanism—are essential for explaining the onset and/or sustainment (*7*–*11*) of longer climate anomalies such as the Little Ice Age (LIA) (ca. 1350 or 1450 to 1850 CE) (*12*). There are, however, differences between and within models in the response to external forcing and nonlinear feedback mechanisms within the climate system. Furthermore, these studies have put forth no comparisons of empirical evidence to support the modeled sea-ice expansion in response to volcanism, with the exception of a single record of the presence of sea ice from North Iceland (*13*) in (*8*). More convincing support for model conjectures requires comparisons with geographically distributed sea-ice records with high temporal resolution to identify abrupt changes. Regional reconstructions of sea-ice extent based on terrestrial proxy networks are inadequate and, moreover, appear to suggest even reduced sea ice during the LIA (*14*).

Empirical evidence of past sea-ice variability from marine archives remains fragmentary, and there are differences in individual reconstructions due to uncertainties in the proxies, as well as chronological issues and, generally, low temporal resolution. Marine sediment cores recording the presence of sea ice from several sites near Greenland have recently become more numerous and with temporal resolution high enough to detect abrupt changes occurring on decadal to century time scales. The advantages of synthesizing sea-ice records from multiple sites have been demonstrated using historical (*15*) and paleoceanographic records (*12*, *16*–*19*).

Here, we synthesize marine-core records to reconstruct the variability of sea ice and polar waters emanating from the Arctic Ocean, exported through Fram Strait and transported toward the North Atlantic through the EGC and offshoot currents during the past 1400 years. The spatial and temporal coverage of these data are commensurate to track the variability and changes across the Medieval Climate Anomaly (MCA) to LIA transition (ca. 1300–1450) (*8*, *12*) and throughout the LIA.

RESULTS

Sea-ice reconstruction

The sea-ice reconstruction is based on paleo-proxy data derived from marine sediment cores containing material indicative of past sea-ice and ocean conditions. These records are based on multiple proxies, including direct sea-ice proxies (e.g., biomarker IP_{25}, a biological compound produced by algae living in sea ice), indirect biological indicators (e.g., foraminifera and diatoms, with certain species more accustomed to colder water conditions), and mineralogical indicators [e.g., ice-rafted debris (IRD), mineral debris incorporated into sea ice during formation in shallow sea regions] (*20*). On the basis of multiple criteria—location, temporal range and resolution, chronological control, and proxy interpretation (see Materials and Methods and the Supplementary Materials)—we evaluated about 25 records and selected 12 records commensurate with the criteria. Eight of the records are within the extended EGC pathway around Cape Farewell and along Southwest/West Greenland, including the end point for the maximum observed extension of Arctic Ocean–origin sea ice ("Storis") along Southwest Greenland (*5*). Four records are also included from sites outside the extended EGC pathway, located beyond the polar front and generally not reached by sea ice (in the modern record) except during major anomalous cold excursions: eastern Fram Strait, central Greenland

[1]NORCE Norwegian Research Centre, Bjerknes Centre for Climate Research, Bergen, Norway. [2]Institute of Arctic and Alpine Research, University of Colorado, Boulder, CO 80309, USA. [3]Geological Survey of Denmark and Greenland, Copenhagen, Denmark. [4]MMT Sweden AB, Västra Frölunda, Sweden.
*Corresponding author. Email: martin.miles@norceresearch.no
†These authors contributed equally to this work.

Sea, and the North Iceland shelf, the latter two influenced by the Jan Mayen Current and the East Icelandic Current, respectively. These outlying records are essential for detecting extreme positive sea-ice anomalies, because sea ice reaches them rarely. The locations of records are shown in Fig. 1, and details are given in Materials and Methods and the Supplementary Materials.

Arctic sea-ice export

To identify anomalies in Arctic sea-ice export, we initially focused on locations near the Fram Strait gateway between Svalbard and Greenland. The nearest core locations are from eastern Fram Strait and the Northeast Greenland shelf, sites that represent primarily sea ice exported from the Arctic Ocean rather than local formation.

The eastern Fram Strait data (cores MSM-5 MSM5/5-712-1 and MSM5/5-723-2) are based on two independent proxies (IP_{25} and IRD), both of which record a major incursion of sea ice in the 1300s (Fig. 2, A and B). The IP_{25} record (*21*) has its highest value in the 1300s, although its century-scale resolution is insufficient to identify a sharp peak or abrupt change. The higher resolution IRD record (*22*) exhibits an abrupt increase around 1300 with elevated values through the 1300s followed by an abrupt decrease in the late 1300s.

The Northeast Greenland records (core PS2641) are based on two independent proxies (IP_{25} and foraminifera), both of which exhibit positive sea-ice anomalies in the 1300s CE. An IP_{25} reconstruction (*21*) has its highest sea-ice biomarker value in the 1300s CE, although this record has century-scale resolution. Recently, higher-resolution reconstructions from the same core have been generated, based on IP_{25} and an independent proxy, the foraminifera *Nonionellina labradorica*, whose relative abundance is interpreted as an indicator of sea ice–related productivity (*23*). The *N. labradorica* abundance reconstruction with subdecadal resolution shows an abrupt increase around 1300 CE, with elevated values for several decades followed by an abrupt decrease in the late 1300s CE (Fig. 2, C and D, blue). This stands out as the singular extreme anomaly (σ +3.3). Furthermore, a recent high-resolution IP_{25} reconstruction from PS2641 also exhibits an abrupt increase in the late 1200s CE (*18*), the largest evident in the 5.2–thousand year (ka) record.

There are remarkable similarities between the eastern Fram Strait and Northeast Greenland records despite their spatial separation and chronological uncertainties. Both of the high-resolution records indicate a near century-scale positive sea-ice anomaly that began abruptly around 1300, peaked in midcentury, and ended abruptly in the late 1300s CE—both records even show the same dip between two maxima separated by ~30 to 40 years (Fig. 2, B and D). The two records also share some similar features of sea-ice variability in subsequent centuries in the LIA, recording four coincident peaks in Arctic sea-ice export between 1600 and the GSA that occurred in the 1960s to 1970s. However, while the eastern Fram Strait IRD record shows an increasing trend from the 1400s onward, the foraminifera record from Northeast Greenland has a slightly decreasing trend (Fig. 2D). The latter may be ascribed to proxy uncertainties, as although the relative abundance of *N. labradorica* is a sensitive marker for pronounced shifts in sea ice and polar waters, it may be less reliable as an indicator of the general background oceanic conditions upon which the sea-ice anomalies are superposed. An independent IP_{25} reconstruction (*18*) from the same site PS2641 indicates a generally positive sea-ice trend during the LIA.

A record from the central Greenland Sea (core PS1878) (*24*) also exhibits a peak in IRD around 1300 CE, which, here, is an unambiguous indicator of a sea-ice incursion (Fig. 2E). Although the century-scale resolution of the record cannot resolve an abrupt change, the IRD peak was exceptional in the past 10 ka of that record, having a σ +2.3 based on the past 2 ka, and coincided with a strong $\delta^{18}O$ peak, indicating the largest freshwater anomaly in the entire Holocene (*24*).

There are thus independent lines of evidence for extreme export of sea ice from the Arctic Ocean in the 1300s CE, unmatched in the millennial-scale records in terms of magnitude (2 to 3 σ) and duration (several decades to near century). Moreover, the high-resolution records demonstrate that both the onset and termination of the sea-ice export anomaly were abrupt, within one to two decades each.

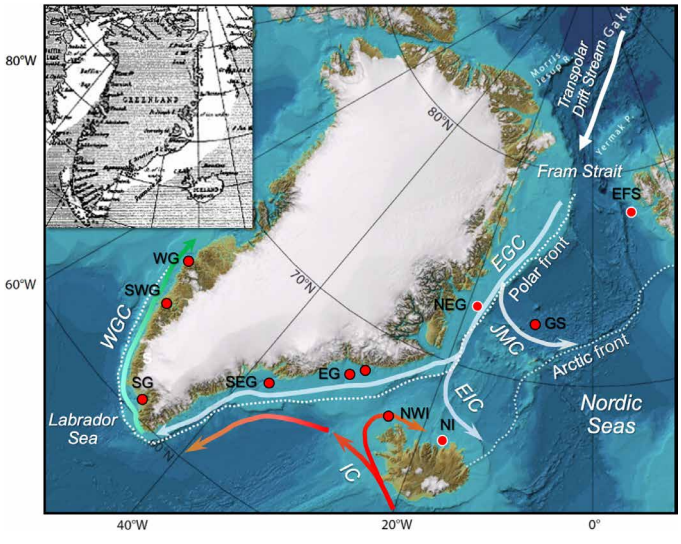

Fig. 1. Oceanographic setting and location of sea-ice proxy records. Bathymetric map of the Fram Strait gateway and downstream region [source: www.ibcao.org (*42*)]. Major surface currents are indicated: EGC, Jan Mayen Current (JMC), East Icelandic Current (EIC), Irminger Current (IC), and West Greenland Current (WGC). Red circles indicate location of marine sediment cores from the eastern Fram Strait (EFS); Greenland Sea (GS); Northeast Greenland (NEG) shelf; northwest Iceland (NWI) shelf; North Iceland (NI) shelf; Kangerdlussuaq and Nansen troughs, East Greenland (EG); Sermilik trough, Southeast Greenland (SEG); Igaliku Fjord, south Greenland (SG); Ameralik Fjord, Southwest Greenland (SWG); and Holsteinborg Dyp, west Greenland (WG). Data records based on the direct sea-ice proxy IP_{25} are outlined in white, and indirect indicators of sea ice and polar waters are outlined in black. Details are given in tables S1 and S2. Inset: Danish historical ice chart from the early 20th century showing the extension of the Arctic Ocean–origin sea ice (Storis) observed along Southwest Greenland (*5*).

Downstream changes in sea ice

Downstream records from the East Greenland shelf in the Denmark Strait [Nansen Trough, core BS-1207 (*25*) and Kangerlussuaq Trough, core MD99-2322 (*26*)] show changes within the EGC pathway contemporaneous with the Arctic sea-ice export anomaly. The Nansen Trough record with bidecadal resolution based on the relative absence of the foraminifera *Cassidulina teretis* as an indicator shows a marked increase in sea ice and polar waters just before 1300 CE of several decades duration culminating around 1370 CE (Fig. 3A). A nearby decadal-resolution record from the Kangerlussuaq Trough (core MD-2322) that reconstructs sea ice based on diatom assemblages (*26*) shows high variability, including an abrupt increase in sea-ice concentration from <30 to >60% in the 1200s CE, with a positive anomaly lasting several decades, concurrent with an abrupt

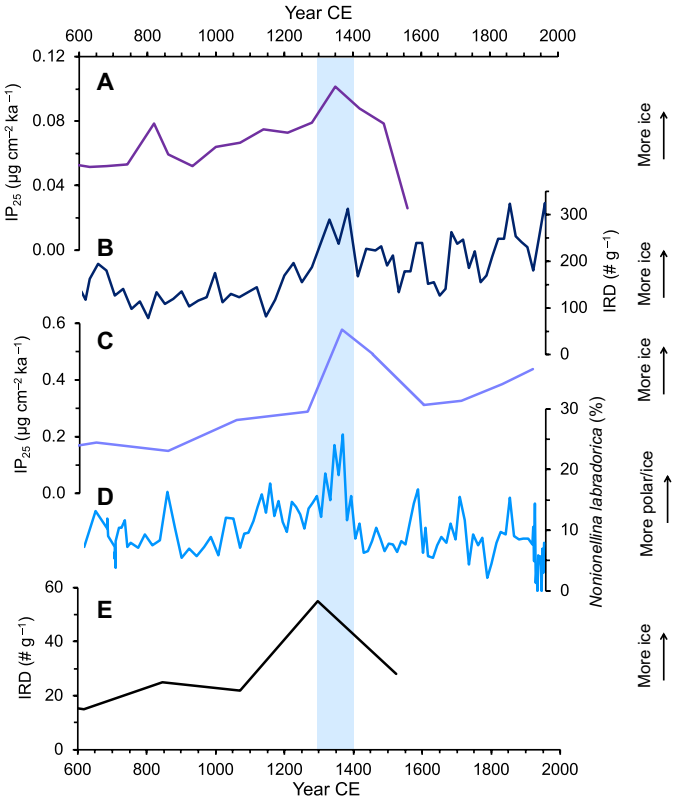

Fig. 2. Arctic sea ice and polar waters from Fram Strait to the Greenland Sea. Sea-ice and ocean reconstructions from marine sediment cores. (**A**) Eastern Fram Strait, based on IP_{25} (*21*). (**B**) Eastern Fram Strait, based on IRD (*22*). (**C**) Northeast Greenland shelf, based on IP_{25} (*21*). (**D**) Northeast Greenland shelf, based on benthic foraminifera (*23*). (**E**) Central Greenland Sea, based on IRD (*24*). Blue shading represents the period of increased sea ice spanning the 1300s CE.

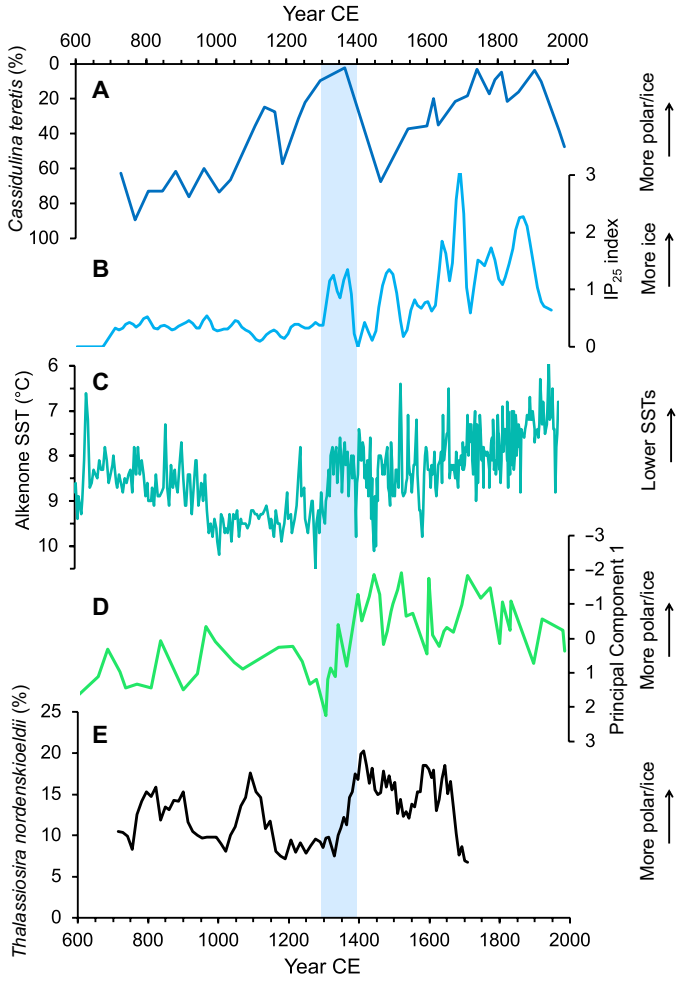

Fig. 3. Arctic sea ice and polar waters downstream in the subarctic North Atlantic. Sea-ice and ocean reconstructions from marine sediment cores: (**A**) Nansen Fjord, East Greenland, based on foraminifera (*25*), inverted scale. (**B**) North Iceland shelf, sea ice based on IP_{25} (*13*). (**C**) North Iceland shelf sea surface temperatures (SSTs) based on alkenones (*29*), inverted scale. (**D**) South Greenland Fjord, based on diatoms (*31*). (**E**) West Greenland shelf, based on diatoms, five-point running average (*33*). Blue shading represents the period of increased polar waters and sea ice spanning the 1300s CE.

shift in diatom fluxes (*27*). On the Southeast Greenland shelf (Sermilik Trough, core Fox04G/05R) (*28*), sedimentological evidence based on grain sizes suggests a greatly intensified EGC transport abruptly arising in the late 1200s CE.

Sea ice appears on Icelandic waters only when there is a large export from the Arctic transported by the EGC and East Icelandic Current. Exceptionally well-dated, high-resolution records from the North Icelandic shelf (core MD-2275) show an abrupt increase in sea-ice proxy IP_{25} values (*13*) beginning in the 1290s CE, concurrent with an abrupt decrease in sea temperatures derived from alkenone biomarker paleothermometry (Fig. 3, B and C) (*29*). The IP_{25} data indicate a positive sea-ice anomaly lasting 60 to 80 years, with a moderate decadal-scale amelioration in the middle of the period, before decreasing abruptly in the late 1300s CE. Afterward, there were largely ice-free conditions in the 1400s CE, until returning to a sustained period of generally more ice from the 1500s to the early 1900s CE. The sea-temperature proxy decreased by 1.5°C during the 1300s CE, and the lower temperatures were sustained for centuries (Fig. 3C). Multiproxy evidence from another marine core from the Northwest Iceland shelf (*30*) also supports the concept of an abrupt ocean-ice regime shift in the 1300s that remained generally sustained for centuries.

Farther downstream in the EGC extension around Cape Farewell, three records along the West Greenland Current (WGC) exhibit changes in the 1300s CE. First, a diatom record from Igaliku Fjord, South Greenland (*31*) shows a rapid increase in sea-ice taxa and EGC influence in the late 1200s, increasing until about 1400 CE (Fig. 3D). Second, a similar shift is evident in diatoms and foraminifera assemblages from a core in Ameralik Fjord, Southwest Greenland (*32*). Third, a record from Holsteinborg Dyb, West Greenland, which represents the end point for Arctic Ocean–origin sea ice along the EGC/WGC pathway, has an abrupt increase in Arctic sea-ice diatoms in the early 1300s CE (Fig. 3E) (*33*). Further support for a regime shift at the Holsteinborg Dyb location comes from benthic foraminifera that indicate a distinct shift from well-mixed to stratified water column and surface flora indicative of sea ice (*34*).

Together, the disparate records from the entire Storis pathway from Fram Strait to Western Greenland show a reasonably coherent signal of a near century-scale sea-ice anomaly that began around 1300 CE, chronological uncertainties notwithstanding. The exceptional magnitude of this "Great Sea-Ice Anomaly" (GSIA) is indicated

by the standardized scores of the anomalies in the 1300s CE. As the sea-ice indicators were on the order of 2 to 3 SDs (σ) above their mean, this anomaly can be considered statistically extreme.

DISCUSSION

Upstream and downstream changes

Although all of the high-resolution records show a change that commenced abruptly in the late 1200s or around 1300 CE, there is a notable difference between the "upstream" records near the Arctic Ocean and "downstream" records along the extended EGC/WGC system (Fig. 4, A and B, respectively). The upstream records representing sea-ice export have a maximum peak in the mid-1300s CE during the sea-ice pulse that ended abruptly in the late 1300s (Fig. 4A). The downstream records—while sharing the abrupt increase in the presence/influence of sea ice and polar waters beginning in the early 1300s CE—are characterized by a steady century-long increase culminating around 1400 CE. Similar to the records upstream, the episode lasted nearly a century, but the maximum values of the polar water and sea-ice proxies occur at the end of the century and are generally sustained from the 1400s CE throughout the LIA into the 1800s, with generally positive σ values (Fig. 4B). The intermediate records (i.e., Denmark Strait and the North Iceland shelf) share characteristics of upstream and downstream records, with a peak in the mid-1300s CE, followed by lower values in the 1400s CE and then generally colder though variable ocean conditions in subsequent centuries until the 20th century.

A plausible explanation for the upstream records displaying a sea-ice peak in the mid-1300s CE while the downstream records are characterized by a steady century-long increase in colder waters and sea ice is that the sea-ice export anomaly cumulatively led to conditioning of the upper ocean downstream, with colder sea-surface temperatures and freshening near the surface. Supporting evidence for a stratified water column is inferred from downstream records from the Southeast (*28*) and Southwest/West (*34*) Greenland shelf.

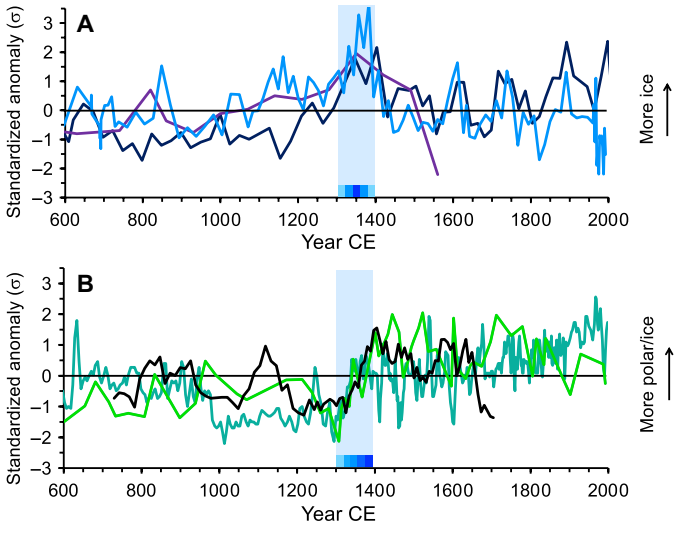

Fig. 4. Comparison of anomalies upstream near the Arctic sea-ice export gateway and downstream anomalies in the subarctic. (**A**) Anomalies (σ units) in sea ice upstream: eastern Fram Strait [purple (*21*) and dark blue (*22*)] and Northeast Greenland [aqua (*23*)]. Blue shading represents the period of increased sea ice peaking in the mid-14th century CE (indigo). (**B**) Anomalies (σ units) in ocean and sea-ice conditions downstream: North Iceland shelf, inverted scale [teal (*29*)], south Greenland [green (*31*)], and west Greenland, five-point running average [black (*33*)]. Blue shading represents the period of increased polar waters and sea ice culminating in the late 1300s CE (indigo).

A relevant question is whether this apparent regime shift along the EGC-WGC system propagated further downstream into the Labrador Sea and, subsequently, led to reduced deep-water formation and a weaker subpolar gyre (SPG) circulation, which has been proposed as a mechanism for initiating LIA-type cooling episodes (*11*, *12*, *16*). Evidence from paleoceanography from the Labrador Sea is, however, not unequivocal with regard to timing. Multiproxy reconstructions from the Eirik Drift in the eastern Labrador Sea south of Greenland show large fluctuations in the 1300s CE, with a shift toward cooling and more polar waters in the second half of the century (*16*, *17*). A separate Mg/Ca temperature reconstruction (*35*) from the same location shows an abrupt cooling and freshening (ΔT ~−1.7°C and ΔS ~0.7 per mil) commencing in the early 1300s CE and reaching its nadir around the end of the century, which mirrors the upstream increases in sea ice and polar waters. Accordingly, the GSIA identified here may have been the specific event that contributed to subsequent changes in the SPG and broader North Atlantic circulation around the onset of the LIA (*12*, *16*).

Initiation of the GSIA

The underlying cause of the initiation of the GSIA is a fundamental question. One explanation is that it was caused by an increase in the frequency and/or magnitude of explosive volcanism beginning in the 1250s CE and a decrease in solar irradiance (e.g., Wolf minimum 1280–1350 CE), as several modeling experiments have studied the role of volcanism and solar forcing in initiating and/or sustaining LIA-like climate anomalies through a cascade of sea-ice feedbacks (*7*–*11*). The timing and abruptness of the sea-ice anomaly described here are consistent with the contention that decadally paced volcanism (fig. S1) could have triggered the initial sea-ice expansion (*8*). However, while "an explanation of the onset of the LIA does not require a solar trigger" (*8*), it may not require a volcanic trigger either. Although forced model runs suggest the sea-ice response to volcanism to be large, abrupt shifts also appear in unforced model runs. Model control simulations have suggested the intriguing possibility that such a large cooling event could arise spontaneously without external perturbation (*36*–*38*). While not identical in the magnitude or duration of the cooling events, independent results from modern, refined models (*37*, *38*) share common features: (i) extreme positive anomalies in sea-ice east off Greenland lasting several decades, (ii) EGC intensification, (iii) anomalous northerly/northwesterly winds east of Greenland associated with a persistent Greenland Blocking pattern, and (iv) further development and enhancement of the cold anomaly through regional sea-ice feedbacks.

These seemingly unrealistic "ugly duckling" (*39*) model results are provocative; however, none of them have been supported with empirical evidence. The most pertinent modeling study (*37*) found a century-scale cooling event in the northern North Atlantic with the same time scale as the GSIA identified here. The modeled sequence matches the spatial and temporal patterns of reconstructed sea-ice anomalies (fig. S2). In the model, positive sea-ice anomalies begin in the Greenland Sea as a result of an abrupt increase in Fram Strait ice export, subsequently enhanced through increased sea-ice growth in the Greenland Sea, which then supported the development of colder ocean and atmospheric conditions leading to atmospheric

circulation anomalies characterized by an increased Greenland Blocking with frequent northerly and northwesterly winds. This eventually led to strongly positive sea-ice anomalies of Southwest Greenland decades after the initial increase in sea-ice export through Fram Strait (*37*). Here, our reconstruction from South and Southwest Greenland (Fig. 3D and fig. S2) also shows an abrupt and steady increase in sea ice and polar waters through the 1300s, reaching a maximum at the end of the century, decades after the midcentury peak seen in the sea-ice records from Fram Strait and Northeast Greenland (Fig. 2, A to D, and fig. S2). Furthermore, from a provenance study of iron oxide grains in the marine core MD99-2263 from Northwest Iceland (*40*), there are also indications of a peak in Arctic Ocean–origin IRD in the late 1200s CE, followed by a peak in East Greenland–origin IRD a few decades later. Arctic Ocean–origin IRD indicates northerly wind, whereas Greenland-origin IRD indicates northwesterly/westerly winds, supporting the modeled atmospheric circulation changes (*37*).

The reconstruction described here provides strong empirical evidence in support of the provocative modeling studies (*36*–*38*) that suggest that abrupt multidecadal to century-scale cooling events can arise spontaneously. This interpretation, however, does not exclude the possibility that external forcing—volcanic and solar—may have contributed to the onset and/or development of LIA conditions, as suggested from forced modeling studies (*7*–*11*). Regardless of the initial cause of the sea-ice expansion, important aspects are the implications of Arctic sea-ice export for the downstream conditions and for sustaining cool periods such as the LIA, underscoring the importance of sea-ice feedbacks in the climate system. Furthermore, our reconstruction provides evidence of an Arctic Ocean–origin sea-ice anomaly that may have contributed to the demise of the Norse colonies in Southwest Greenland in the 14th and 15th centuries CE (*38*). Last, our finding of extreme export of Arctic sea ice leading to a sustained cooling period also has important implications for predicting Arctic climate change. In a warming future climate with reduced sea ice, GSA-like events will be important, as frequent purges of sea ice and freshwater from the Arctic Ocean driven by anomalous winds are anticipated (*41*).

MATERIALS AND METHODS

Data records

The paleo-data records analyzed here were derived from marine sediment cores using various proxies indicative of sea-ice and ocean conditions (*20*). Four strict evaluation criteria were used for selecting the records for inclusion from those available: (i) Spatial location within the polar front (Fig. 1) where sea ice and polar waters are generally present or within the Arctic front reached by Arctic origin sea ice under anomalous conditions; if there are several nearby cores, e.g., North Iceland shelf, then only one or two records were selected (based on the other criteria) to represent the location; (ii) temporal coverage extending back at least one millennium, i.e., covering the transition from the MCA to LIA, preferably with decadal-to-century temporal resolution; (iii) chronological control constrained with at least four radiocarbon dates in the past millennium; and (iv) proxies with demonstrated ability to record the presence of sea ice and/or polar waters, preferably with multiple proxies from the same core.

On the basis of these criteria, we selected 12 commensurate records (i) spanning the length of the extended EGC pathway from Fram Strait to Cape Farewell and the WGC, with the Holsteinborg Dyb record (WG in Fig. 1) being the northernmost end member for the extension of the Arctic sea ice along west Greenland, and (ii) located beyond the polar front (including the Jan Mayen Current and East Icelandic Current) including "end members" for maximum sea-ice excursions: east Fram Strait, central Greenland Sea, and North Iceland, locations not generally reached by Arctic sea ice in modern record except for anomalous situations such as the GSA. The locations of the records are shown in Fig. 1, and details are given in tables S1 and S2.

Climatic interpretation of proxies

Several different proxies for sea ice and polar waters are included, both direct sea-ice proxies (IP_{25}) from three sites and indirect proxies for sea ice and polar waters from several sites. South of Denmark Strait, no IP_{25} reconstructions are available, so indirect proxy indicators of sea ice and polar waters are used. The original interpretations of the authors are maintained. While each record is based on measured quantities, the proxies represent the relative presence or absence of sea ice and polar waters rather than geophysical quantities. These are, however, scalar quantities that are amenable to qualitative analysis and objective comparison of the magnitude of changes using standardized anomalies.

Age control

No adjustments were made to the temporal resolution or chronologies of the individual records, whose characteristics are summarized in tables S1 and S2. The century-scale resolution records were used to flag anomalies that were then studied further using high-resolution (decadal) records. The high-resolution records also have better age control, particularly those dated with precise markers such as tephra (*13*, *29*), allowing the onset, duration, and magnitude of changes in sea-ice and ocean characteristics to be identified. Comparison between sediment cores is limited by the inherent lack of absolute, accurate dating; however, the characteristics of the GSIA and smaller distinctive anomalies seen in subsequent centuries match remarkably well not only in duration but also in timing within a decade or two. Together, the high-resolution records from multiple sites around the EGC system strongly suggest a contemporaneous event.

SUPPLEMENTARY MATERIALS

Supplementary material for this article is available at http://advances.sciencemag.org/cgi/content/full/6/38/eaba4320/DC1

REFERENCES AND NOTES

1. IPCC, *Climate Change 2013: The Physical Science Basis*, T. F. Stocker, D. Qin, G.-K. Plattner, M. Tignor, S. K. Allen, J. Boschung, A. Nauels, Y. Xia, V. Bex, P. M. Midgley, (Cambridge Univ. Press, 2013), pp. 953–1028.
2. M. Mori, M. Watanabe, H. Shiogama, J. Inoue, M. Kimoto, Robust Arctic sea-ice influence on the frequent Eurasian cold winters in past decades. *Nature Geosci.* **7**, 869–873 (2014).
3. T. Vihma, Effects of Arctic sea ice decline on weather and climate: A review. *Surv. Geophys.* **35**, 1175–1214 (2014).
4. R. R. Dickson, J. Meincke, S.-A. Malmberg, A. J. Lee, The "Great Salinity Anomaly" in the northern North Atlantic 1968–1982. *Prog. Oceanogr.* **20**, 103–151 (1988).
5. T. Schmith, C. Hansen, Fram Strait ice export during the nineteenth and twentieth centuries reconstructed from a multiyear ice index from southwestern Greenland. *J. Climate* **16**, 2782–2791 (2003).
6. R. Zhang, G. K. Vallis, Impact of Great Salinity Anomalies on the low-frequency variability of the North Atlantic climate. *J. Climate* **19**, 470–482 (2006).
7. Y. Zhong, G. H. Miller, B. L. Otto-Bliesner, M. M. Holland, D. A. Bailey, D. P. Schneider, Á. Geirsdóttir, Centennial scale climate change from decadally-paced explosive volcanism: A coupled sea ice-ocean mechanism. *Clim. Dynam.* **37**, 2373–2387 (2011).

8. G. H. Miller, Á. Geirsdóttir, Y. Zhong, D. J. Larsen, B. L. Otto-Bliesner, M. M. Holland, D. A. Bailey, K. A. Refsnider, S. J. Lehman, J. R. Southon, C. Anderson, H. Björnsson, T. Thordarson, Abrupt onset of the Little Ice Age triggered by volcanism and sustained by sea-ice/ocean feedbacks. *Geophys. Res. Lett.* **39**, L02708 (2012).
9. F. Lehner, A. Born, C. C. Raible, F. Stocker, Amplified inception of European Little Ice Age by sea ice–ocean–atmosphere feedbacks. *J. Climate* **26**, 7586–7602 (2013).
10. E. Moreno-Chamarro, D. Zanchettin, K. Lohmann, J. H. Jungclaus, An abrupt weakening of the subpolar gyre as trigger of Little Ice Age-type episodes. *Clim. Dynam.* **48**, 727–744 (2017).
11. C.-F. Schleussner, G. A. Feulner, A volcanically triggered regime shift in the subpolar North Atlantic Ocean as a possible origin of the Little Ice Age. *Clim. Past* **9**, 1321–1330 (2013).
12. P. Moffa-Sánchez, E. Moreno-Chamarro, D. J. Reynolds, P. Ortega, L. Cunningham, D. Swingedouw, D. E. Amrhein, J. Halfar, L. Jonkers, J. H. Jungclaus, K. Perner, A. Wanamaker, S. Yeager, Variability in the northern North Atlantic and Arctic oceans across the last two millennia: A review. *Paleoceanogr. Paleoclim.* **34**, 1399–1436 (2019).
13. G. Massé, S. J. Rowland, M.-A. Sicré, J. Jacob, E. Jansen, S. T. Belt, Abrupt climate changes for Iceland during the last millennium: Evidence from high resolution sea ice reconstructions. *Earth Planet. Sci. Lett.* **269**, 565–569 (2008).
14. C. Kinnard, C. M. Zdanowicz, D. A. Fisher, E. Isaksson, A. de Vernal, L. G. Thompson, Reconstructed changes in Arctic sea ice over the past 1,450 years. *Nature* **479**, 509–512 (2011).
15. M. W. Miles, D. V. Divine, T. Furevik, E. Jansen, M. Moros, A. E. J. Ogilvie, A signal of persistent Atlantic multidecadal variability in Arctic sea ice. *Geophys. Res. Lett.* **41**, 463–469 (2014).
16. P. Moffa-Sánchez, I. R. Hall, S. Barker, D. J. R. Thornalley, I. Yashayaev, Surface changes in the eastern Labrador Sea around the onset of the Little Ice Age. *Paleoceanogr. Paleocl.* **29**, 160–175 (2014).
17. M. Alonso-Garcia, H. F. Kleiven, J. F. McManus, P. Moffa-Sanchez, W. S. Broecker, B. P. Flower, Freshening of the Labrador Sea as a trigger for Little Ice Age development. *Clim. Past* **13**, 317–331 (2017).
18. H. M. Kolling, R. Stein, K. Fahl, K. Perner, M. Moros, Short-term variability in late Holocene sea ice cover on the East Greenland Shelf and its driving mechanisms. *Palaeogeogr. Palaeoclim. Palaeoecol.* **485**, 336–350 (2017).
19. P. Moffa-Sánchez, I. R. Hall, North Atlantic variability and its links to European climate over the last 3000 years. *Nature Comms.* **8**, 1726 (2017).
20. A. de Vernal, R. Gersonde, H. Goosse, M.-S. Seidenkrantz, E. W. Wolff, Sea ice in the paleoclimate system: The challenge of reconstructing sea ice from proxies – an introduction. *Quat. Sci. Rev.* **79**, 1–8 (2013).
21. J. Müller, K. Werner, R. Stein, K. Fahl, M. Moros, E. Jansen, Holocene cooling culminates in sea ice oscillations in Fram Strait. *Quat. Sci. Rev.* **47**, 1–14 (2012).
22. K. Werner, R. F. Spielhagen, D. Bauch, H. C. Hass, E. Kandiano, K. Zamelczy, Atlantic Water advection to the eastern Fram Strait – Multiproxy evidence for late Holocene variability. *Palaeogeogr. Palaeoclimatol. Palaeoecol.* **308**, 264–276 (2011).
23. K. Perner, M. Moros, J. M. Lloyd, E. Jansen, R. Stein, Mid to late Holocene strengthening of the East Greenland Current linked to warm subsurface Atlantic water. *Quat. Sci. Rev.* **129**, 296–307 (2015).
24. M. M. Telesiński, R. F. Spielhagen, E. M. Lind, A high resolution Late Glacial and Holocene paleoceanographic record from the Greenland Sea. *Boreas* **43**, 273–285 (2014).
25. A. E. Jennings, N. J. Weiner, Environmental change on eastern Greenland during the last 1300 years: Evidence from foraminifera and lithofacies in Nansen Fjord, 68°N. *Holocene* **6**, 179–191 (1996).
26. A. Miettinen, D. V. Divine, K. Husum, N. Koç, A. Jennings, Exceptional ocean surface conditions on the SE Greenland shelf during the Medieval Climate Anomaly. *Paleoceanogr. Paleoclimatol.* **30**, 1657–1674 (2015).
27. A. Justwan, N. Koç, A. Jennings, Evolution of the East Greenland Current between 1150 and 1740 AD, revealed by diatom-based sea surface temperature and sea-ice concentration reconstruction. *Polar Res.* **28**, 165–176 (2009).
28. C. S. Andresen, M. J. Hansen, M.-S. Seidenkrantz, A. E. Jennings, M. F. Knudsen, N. Nørgaard-Pedersen, N. K. Larsen, A. Kuijpers, C. Pearce, Mid- to late-Holocene oceanographic variability on the Southeast Greenland shelf. *Holocene* **23**, 167–178 (2012).
29. M.-A. Sicré, I. R. Hall, J. Mignot, M. Khodri, U. Ezat, M.-X. Troung, J. Eiriksson, K.-L. Knudsen, Sea surface temperature variability in the subpolar Atlantic over the last two millennia. *Paleoceanogr. Paleoclimatol.* **26**, PA4218 (2011).
30. J. T. Andrews, S. T. Belt, S. Olafsdottir, G. Massé, L. L. Vare, Sea ice and marine climate variability for NW Iceland/Denmark Strait over the last 2000 cal. yr BP. *Holocene* **19**, 775–784 (2009).
31. K. G. Jensen, A. Kuijpers, N. Koç, J. Heinemeier, Diatom evidence of hydrographic changes and ice conditions in Igaliku Fjord, South Greenland, during the past 1500 years. *Holocene* **14**, 152–164 (2004).
32. M.-S. Seidenkrantz, S. Aagaard-Sørensen, H. Sulsbrück, A. Kuijpers, K. G. Jensen, H. Kunzendorf, Hydrography and climate of the last 4400 years in a SW Greenland fjord: Implications for Labrador Sea palaeoceanography. *Holocene* **17**, 387–401 (2007).
33. L. Sha, H. Jiang, K. L. Knudsen, Diatom evidence of climatic change in Holsteinborg Dyb, west of Greenland, during the last 1200 years. *Holocene* **22**, 347–358 (2011).
34. D. R. Erbs-Hansen, K. L. Knudsen, J. Olsen, H. Lykke-Andersen, J. A. Underbjerg, L. Sha, Paleoceanographical development off Sisimiut, West Greenland, during the mid- and late Holocene: A multiproxy study. *Marine Micropaleont.* **102**, 79–97 (2013).
35. H. F. Kleiven, I. V. Johansen, U. Ninnemann, North Atlantic climate and deep water variability since 600 AD. *IOP Conf. Ser. Earth Environ. Sci.* **6**, 072036 (2009).
36. A. Hall, R. J. Stouffer, An abrupt climate event in a coupled ocean–atmosphere simulation without external forcing. *Nature* **409**, 172–174 (2001).
37. S. Drijfthout, E. Gleeson, H. A. Dijkstra, V. Livina, Spontaneous abrupt climate change due to an atmospheric blocking-sea-ice-ocean feedback in an unforced climate model simulation. *Proc. Natl. Acad. Sci. U.S.A.* **110**, 19713–19718 (2013).
38. E. Moreno-Chamarro, D. Zanchettin, K. Lohmann, J. H. Jungclaus, Internally generated decadal cold events in the northern North Atlantic and their possible implications for the demise of the Norse settlements in Greenland. *Geophys. Res. Lett.* **42**, 908–915 (2015).
39. C. Li, A. Born, Coupled atmosphere-ice-ocean dynamics in Dansgaard–Oeschger events. *Quat. Sci. Rev.* **203**, 1–20 (2019).
40. D. A. Darby, W. Myers, S. Herman, B. Nicholson, Chemical fingerprinting, a precise and efficient method to determine sediment sources. *J. Sediment. Res.* **85**, 247–253 (2015).
41. T. W. N. Haine, B. Curry, R. Gerdes, E. Hansen, M. Karcher, C. Lee, B. Rudels, G. Spreen, L. de Steur, K. D. Stewart, R. Woodgate, Arctic freshwater export: Status, mechanisms, and prospects. *Global Planet. Change* **125**, 13–35 (2015).
42. M. Jakobsson, L. Mayer, B. Coakley, J. A. Dowdeswell, S. Forbes, B. Fridman, H. Hodnesdal, R. Noormets, R. Pedersen, M. Rebesco, H. W. Schenke, Y. Zarayskaya, D. Accettella, A. Armstrong, R. M. Anderson, P. Bienhoff, A. Camerlenghi, I. Church, M. Edwards, J. V. Gardner, J. K. Hall, B. Hell, O. Hestvik, Y. Kristoffersen, C. Marcussen, R. Mohammad, D. Mosher, S. V. Nghiem, M. T. Pedrosa, P. G. Travaglini, P. Weatherall, The International Bathymetric Chart of the Arctic Ocean (IBCAO) Version 3.0. *Geophys. Res. Lett.* **39**, L12609 (2012).
43. C. Gao, L. Oman, A. Robock, G. L. Stenchikov, Atmospheric volcanic loading derived from bipolar ice cores: Accounting for the spatial distribution of volcanic deposition. *J. Geophys. Res.* **112**, D23111 (2007).
44. F. Steinhilber, J. Beer, C. Fröhlich, Total solar irradiance during the Holocene. *Geophys. Res. Lett.* **36**, L19704 (2009).

Acknowledgments: We thank all the research groups for producing and providing public access to their sea-ice proxy records. We thank K. Perner for contributing data from the Northeast Greenland shelf and the helpful discussions. We thank the two anonymous reviewers and M. A. Kelly for constructive comments, leading to improvement of the manuscript. **Funding:** This research received funding from the European Research Council under the European Community's Seventh Framework Programme (FP7/2007-2013)/ERC grant agreement 610055 as part of the ice2ice project. Funding support has also been provided by the Norwegian Research Council (Norges Forskningsråd grant no. 231531 "EASTGREEN" and grant no. 263053 "ULTRAMAR"), the Centre for Climate Dynamics at the Bjerknes Centre, and the Danish VILLUM Foundation for the project "Past and future dynamics of the Greenland Ice Sheet" (grant no. 10100). **Author contributions:** M.W.M. initiated and led the work. C.V.D. collected and evaluated the data records. M.W.M. and C.S.A. interpreted the results and wrote the manuscript. All authors contributed to the final manuscript. **Competing interests:** The authors declare that they have no competing interests. **Data and materials availability:** All data needed to evaluate the conclusions in the paper are present in the paper and/or the Supplementary Materials. Additional information related to this paper may be requested from the authors.

Submitted 3 December 2019
Accepted 29 July 2020
Published 16 September 2020
10.1126/sciadv.aba4320

Citation: M. W. Miles, C. S. Andresen, C. V. Dylmer, Evidence for extreme export of Arctic sea ice leading the abrupt onset of the Little Ice Age. *Sci. Adv.* **6**, eaba4320 (2020).

Evidence for extreme export of Arctic sea ice leading the abrupt onset of the Little Ice Age

Martin W. Miles, Camilla S. Andresen and Christian V. Dylmer

Sci Adv **6** (38), eaba4320.
DOI: 10.1126/sciadv.aba4320